University of Utah
UNDERGRADUATE RESEARCH JOURNAL

MANAGING CHRONIC MUSCULOSKELETAL PAIN WITH COMBINED MODALITIES IN NANOXENE AND THERMALLY RESPONSIVE POLYMER NETWORKS

Jesus Manuel Gomez (Dr. Feng Liu)

Department of Materials Science and Engineering

Abstract

This paper describes the design and prototyping of a biomedical device for the management of pain from chronic musculoskeletal conditions. The device incorporates thermotherapy with a heating element that emits infrared radiation. The heating element is made of Nanoxene, a lightweight and moldable material capable of efficiently heating uniform surface areas. It is combined with a hydrogel layer and optimized with molecular imprinting for transdermal drug diffusion. The methodologies behind designing stimuli responsive hydrogels as well as testing their release kinetics are discussed. The hydrogel layer utilizes a copolymer cross-linked matrix consisting of NIPAam, butenediol, and EGDMA. It is cross-linked using an APS-TEMED initiator complex. The hydrogel polymer matrix is made responsive to thermal stimulus. Samples are loaded into heated cuvettes for UV-Vis spectrophotometry testing. The release kinetics with respect to temperature response show a clear correlation with temperature increase. Rheology measurements are performed with a slip rheometer to define the shear modulus, and average cross linking density for the hydrogels. This paper also describes the design of a thermostat switch to control the Nanoxene heating element using an Arduino. Programming the switch with boolean logic selection structures allows for the definition of operational modes as well as increases in battery life. In effect, this device aims to deliver pain relief through a combination of thermotherapy and localized transdermal drug diffusion. The heating element and the hydrogel ameliorate the purpose of one another. It is shown that, under elevated temperatures of approximately 45 °C, the hydrogels exhibit a notable release of solute molecules which is detected through increases in absorbance using UV-Vis spectrophotometry. This is shown to be an ideal operating temperature for the combined benefits of transdermal drug diffusion and thermotherapy.

Introduction

Medical professionals currently treat pain, depending on its severity and nature, by using surgery, analgesic medication, or with rehabilitative therapy. This may involve prosthetics for life, or lifelong visits to a chiropractor or physiatrist at a physical rehabilitation clinic[1][2]. This commonly ends in situations where the procedures taken were more traumatizing to an area with too much being done, or not enough being done to treat the patient's level of pain. Patients are then left with chronic pain that is often treated with addictive medication that leaves the patient with a chemical dependency, like with analgesics derived from opioids. These analgesics are administered now with long term release hydrogel patches like Fentanyl, however these patches lack tunability in their release kinetics, diffusing more slowly as the concentration depletes.

Alternative approaches to managing pain consist of over the counter remedies which are typically ineffective. These include tinctures, creams, and devices that vibrate and provide massages with resistive heating coils. Tinctures and creams used to heat and cool affected areas only provide the sensation of heating and cooling from using capsaicin and other similar chemicals[3]. They provide this sensation by the stimulation of free nerve endings and the dilation of blood vessels in tissues, which does raise the temperature of the body locally[3]. They do not, however provide genuine heat[1][2]. Heating pads such as hot water bottles have traditionally provided inexpensive heat, though they do not offer the tunability of other electrical devices on the market. The current electrical devices used implement wasteful and inefficient heating coils that do not provide uniform heat to the affected area. Heating coils are also bulky, unwieldy, and are dangerous as they are prone to short circuit failures.

Where these approaches fail in managing pain, a device that integrates the best qualities of each individual approach - a device with a heating element that diffuses medicine locally - may succeed in delivering targeted pain relief. This device could treat pain without prescribing large doses of analgesic pain medication that may leave a patient addicted. Therefore, there exists a need for a device which may deliver medication locally to an area via transdermal drug diffusion while simultaneously providing heat to an area to relieve pain. Such a device could be designed to be portable so patients could use it throughout their day and modular such that the heating element and diffusive medicine layer are separable yet combinable. The challenges to designing such a device are:

1. Design a hydrogel surface layer with desirable release kinetics and viscoelastic properties for use as a transdermal drug diffusion system.
2. Design a flat, lightweight, and portable heating element that is powered safely, is more efficient than traditional heating coils, and could be controlled with a simple interface for a patient to operate without medical supervision.
3. Design a scheme which will conserve power or battery life for optimal use during extended periods of time.
4. Integrate into the device a self responsive feedback system to deactivate under high heat which could harm a patient.

Fulfilling these criteria segues into a fully functioning prototype. The real value of this device comes from the integration of the combined modalities of each individual approach. First, thermotherapy provides activation energy which aids transdermal drug diffusion into the body. This follows directly from the kinetics of diffusion and Fick's First Law of Diffusion[4].

Secondly, a hydrogel that is thermally responsive delivers increased amounts of medicine under higher operating temperatures[5]-[8]. Finally, utilizing a hydrogel with thermotherapy ameliorates the diffusion of heat through tissues in the body as the water trapped in the hydrogel has a much higher thermal conductivity than air does[9]. This air would sit between the heating element and skin, providing a larger barrier for heat transfer into the body, lowering the efficiency of the heating element.

The final effort is in the integration of each individual subsystem into a fully functioning device for further prototyping and testing. The final prototype before mass production is then further optimized through the miniaturization of the electronic components to reduce the costs of fabrication, for example. This concern did not fit into the scope of this design project, though. Given that larger companies have more experience with concerns like those than the University of Utah does, this project focuses solely on the rapid prototyping and design processes behind the typical devices that consumers use daily.

Product Design and Specifications

Overview of Subsystems

There are a total of four subsystems: the thermally responsive hydrogel, the Nanoxene heating element, the integrated circuitry, and the push button and LED display that run the circuitry. The hydrogel will be in contact on one end with skin and on the other end with Nanoxene. The hydrogel to Nanoxene adhesive layer connection is the initial interface of the total system. The next interface is that of the Nanoxene heating element with the integrated circuit. Finally, the last interface is that of the microcontroller program with the integrated circuit and the push button controls and LEDs. Refer to illustration 1 for an overview of the subsystems in a flowchart diagram.

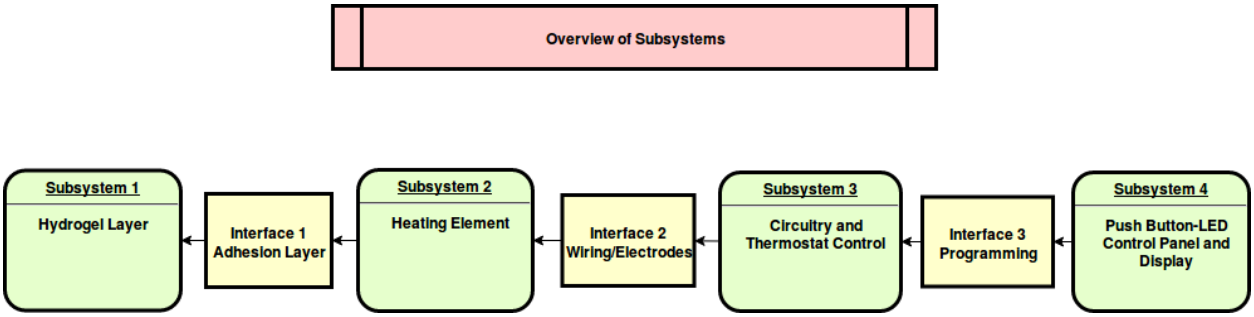

Illustration 1: A layout of the subsystems and their pathways of control

The first subsystem design of the hydrogel has to be optimized for thermal stimulus responsivity, mechanical properties, and molecular imprinting of medication. This thermal stimulus is controlled by selecting monomers that exhibit the required response. This may be expansion, contraction, or color change among various other responses. When a hydrogel contracts under heat, it will increase its internal osmotic pressure and drive an increase in diffusivity of solution out of the polymer matrix. NIPAam has demonstrated this behavior by changing its conformational state under heat such that it contracts the entire hydrogel when polymerized. These changes in conformation are known as coil to globular transitions and are common in proteins that also have amide groups in their peptide monomers[5]-[8].

The hydrogel must be mechanically sound such that the hydrogel won't tear under use. This is controlled mainly through the polymerization reaction initial conditions. Low amounts of initiator complex for longer polymerization times leads to long range chain growth and greater mechanical strength. Using higher temperatures will reduce the required time for polymerization. However, higher temperatures reduces the likelihood of successful molecular imprinting in the hydrogel[10]. This is because molecular imprinting requires an organization of monomers in solution around target molecules through Van-Der-Waals attraction forces prior to polymerization. When the polymerization occurs, these monomers are polymerized in place in a unique conformational scheme which only fits the target molecules. These serve as docking centers which the medicine can fit into and allow for higher concentrations of medicine once loaded. At higher temperatures, polymerizations occur rapidly at the expense of decomposing the attractive forces necessary for molecular imprinting. It may be the case that molecular imprinting is simply not necessary. An efficient and pragmatic approach to mass production of these hydrogels may be preferable. Extensive testing is required to flesh out a solution.

The hydrogel/Nanoxene interface must have similar thermal conductivity in order to transport heat effectively and must be elastic so that it is capable of molding to various body types. The elasticity is proposed by using gum adhesives and expandable fabrics for base materials. Although the hydrogel may reliably have the necessary elastic characteristics, Nanoxene may not. The Nanoxene heating element subsystem can be tape cast onto a variety of substrates and is relatively inexpensive to make. The only problem with using elastic materials is that Nanoxene requires a conductive material for electrodes such as copper tape. The copper tape is not very elastic and will fail if it is stretched beyond its fracture point. Care must be taken to implement copper leads with pleats or expandable geometries in the wiring interface. Copper wires could even be woven into more expensive fabrics.

The circuitry subsystem and wiring interface with Nanoxene is the most crucial interface and subsystem. It regulates temperature, and battery consumption and is the area of main concern for risk of burns and shock. Controlling the circuit interface with TIP-120 transistors will provide the necessary factor of safety for avoiding risks from overheated transistors failing to provide the necessary power for operation. TIP-120 transistors have max voltage and current ratings of 60 V and 14 A which is well above what Nanoxene requires to operate. Laminating Nanoxene in mylar sheets, as aforementioned, would go a long way towards preventing frays and electric shock. The battery which will power Nanoxene in the circuitry subsystem has to be small enough to be integrated into the device without limiting flexibility and comfort. Additionally, the power consumption of the device has to be low enough so that it could last for extended operating times.

Finally, the last interface is for the circuitry and microcontroller programming connection to the push button and LED control panel subsystem. The circuitry will include a user interface subsystem as a push button to choose operational modes and a few LEDs to let the user know how the device is doing. A more advanced device could use an LCD display to show current operational modes and temperatures. All of these components will be set on a breadboard during prototyping. The microcontroller has inputs from the circuitry on analog pins to read temperature data from sensors and the push button. The outputs from the board are all on digital pins and control the transistor switch in the circuit. The programming interface is what allows the microcontroller to take these inputs and convert them to operations and control outputs. The programming loaded onto the microcontroller is prepared with Arduino C+, the programming

language for Arduino boards. It utilizes boolean selection structures that can be pre-defined to control the device. A boolean selection structure uses logic and read data from pins to decide what operation to perform. This way, if the temperature is above or below a certain range, and if a push button counter reads a certain value the microcontroller will decide whether or not to send power to the transistor. Temperature ranges are easily set in the program and can be fixed such that no one can alter them, and potentially harm themselves.

Project Plan and Procedure

Hydrogel Synthesis and Characterization

All chemicals were ordered from Sigma-Aldrich and used as received in the polymerizations. NIPAam (N-isopropyl acrylamide) (CAS 2210-25-5) has shown LCST values in a range of 32 to 45 °C , which is a similar range to that of human body temperature. Using a copolymer with NIPAam was also shown to vary the LCST depending on the combination of monomers used. After some review, butenediol (cis-[1,4]-2-butenediol) (CAS 6117-80-2) was chosen to pair with NIPAam. It is relatively inexpensive given its small size and simple synthesis, and has two hydroxyl groups per monomer. In order to cross-link the hydrogel, any monomer with two functional groups capable of polymerization is all that is needed. EGDMA (ethylene glycol dimathacrylate) (CAS 97-90-5) cross linkers were used to bond the chains into an elastomeric hydrogel. EGDMA has the added benefit of being water soluble from the carbonyl groups on its molecular structure. APS (ammonium persulfate) (CAS 7727-54-0) initiator and TEMED (N,N,N,N-tetraethylmethylenediamine) (CAS 110-18-9) catalyst were used as the initiator complex for the hydrogels as they are water soluble, fast, and inexpensive.

Molar ratios ranging from 90:10 to 99:1 NIPAam to butenediol were implemented. These ratios were considered from the literature review of other successful NIPAam hydrogels in an attempt to optimize the properties of this set of monomers. Ratios of 95:5 to 99:1 NIPAam to EGDMA were investigated for ideal cross-linking and mechanical strength optimization. The formation of the polymer network utilizes free radical polymerization with APS and TEMED[11]. APS was selected since it is a thermally activated initiator that dissociates at room temperature in the proper solvent. To make long chains for a strong hydrogel, very little initiator is needed since the probability of a growing chain being terminated by another is lowered. This polymerization used TEMED as a catalyst at $1:7.5x10^{-2}$ NIPAam to TEMED and APS at $1:1x10^{-3}$ NIPAam to APS. This ratio provides ideal polymerization times for both room temperature to hot polymerizations. Polymerization temperatures were investigated at room temperature and at high temperatures of approximately 50 °C, near the melting point of NIPAam. This was to test effects on polymerization time and molecular imprintability. Three solvents were investigated here for their interaction characteristics: water, acetone, and THF. This was to see which works best for ideal miscibility in pre-gel solutions. Refer to table 1 below for pertinent information to the molar and sample ratios used to make the hydrogels.

Reagent	%mol	Weight	Volume	Concentration
NIPAam	95	1.07 g		Dissolve into $500x10^{-3}$ mL solvent
butenediol	5		$41.0x10^{-3}$ mL	
EGDMA	1.5		$28.2x10^{-3}$ mL	
TEMED	$7.5x10^{-3}$		$112.5x10^{-3}$ mL	
APS	$1.0x10^{-3}$	$17.12x10^{-3}$ g		Dissolve into $500x10^{-3}$ mL
Lidocaine+HCl 5%		5 g		Dissolve into H_2O 500 mL (pH 6)

Table 1: A collection of reagent concentrations used in the polymerization. Two pre-gel solutions were mixed: one was the pre-polymerization mix and the other was the initiator complex mix. In order to make samples, a 1:1 ratio of each solution were mixed together.

Testing the hydrogels is done once the samples are fully washed, cycled, and loaded. A solution of lidocaine + HCl 5% was prepared to test the loading characteristics and release kinetics of the samples. The release kinetics testing involves analyzing UV-Vis data on absorbance, referred to as A, over time and with changes in temperature. This elucidates the release of medicine from the hydrogel from the change in concentration over time inside the cuvette. Samples are loaded into cuvettes, and tested using UV-Vis scans every 5 minutes. At 20 minutes, the cuvettes are placed in a hot water bath at approximately 45 ^{o}C, and tested again every 5 minutes with another heating cycle before each scan. The analysis involves using the Beer-Lambert Law to convert the absorbance data to concentration. Using the molar absorptivity of a known substance in solution, referred to as ε, and the interaction length of the light with the cuvette, referred to as l, data on absorbance can be converted to concentrations. Once the data is integrated using numerical methods such as trapezoidal integration, the total concentration, referred to as c, with respect to time and temperature can be derived. Refer to equations one and two for the definitions of the Beer-Lambert law and Absorbance below. They illustrate the models used to solve for total concentration.

The viscoelastic behavior of the hydrogels is measured by using a slip rheometer. This machine uses dynamic strain testing to test rheometry in the samples with respect to frequency. The machine applies torsional strain for varying frequencies to uniform hydrogel disks of radius r, and thickness t to derive the elastic shear modulus, referred to as G. Using the length, referred to as L, the disk inertia, referred to as I_d, the applied torsion required to illicit shear stress, referred to as T, and the strain angle, referred to as φ, the derivation of the shear modulus G can be done for static loading measurements within the domain of yielding forces in a material[12].

Furthermore, when the strain rate, traditionally referred to as γ, is varied with cyclical frequency, referred to here as ω, data on the loss tangent, or the tangent of the phase angle, referred to as δ, can be defined. This first involves converting the data on the measured shear modulus to the complex domain and modeling a sample's response with polar phase angles. The real component of the shear modulus here is called the storage modulus, and is referred to as G'. The imaginary component of the shear modulus here is called the loss modulus, and is referred to as G''. Using these data, the sample volume, referred to as V, and the thermal activation energy k_bT, an average cross-linking density in the hydrogel sample, referred to as N_s, can be derived.

A material with little to no loss modulus, low loss tangents, and a constant storage modulus, would be considered near perfectly elastic in the dynamic frequency range considered. Conversely, a material with nearly pure loss, high loss tangents, and a low storage modulus would be considered near perfectly viscous. Most polymeric materials have responses that are usually somewhere in between the two regimes, or viscoelastic responses. Refer to equations three, four, five, and six for the definitions of the torsional shear modulus, complex shear, the loss tangent, and cross linking density below. They illustrate the models used to solve for the mechanical properties of hydrogel samples.

$$A = \log_{10} \frac{I_f}{I_i}$$ eq. 1 (A*bsorbance as attenuation of intensity relationship*)

$$A = \varepsilon\, lc$$ eq. 2 (*Beer-Lambert Law relationship for absorbance and concentration*)

$$G = \frac{T\,L}{\phi\, I_d}$$ eq. 3 (S*tatic torsional shear modulus relationship*)

$$G = G' + iG'' = \frac{\tau_o}{\phi_o} e^{i\delta}$$ eq. 4 (C*omplex representation of dynamic shear*)

$$G = \frac{N_s}{V} k_b T$$ eq.5 (C*ross linking density relationship*)

$$\tan(\delta) = \frac{G''}{G'}$$ eq. 6 (R*elationship for loss tangent and complex modulus*)

butenediol

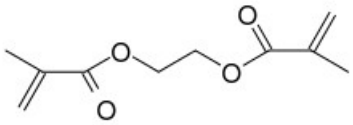

EGDMA

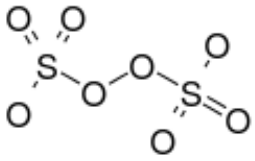

APS

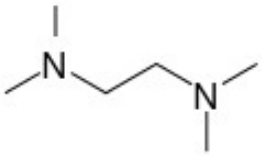

TEMED

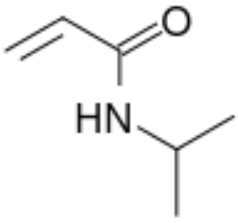

NIPAam

Illustration 2: All the monomers used in this polymerization are displayed here. The functional group necessary for polymerization is the alkene double bond. EGDMAs two alkenes are what cross-links chains with physical bonds. The hydroxyl groups on butenediol are what provide the hydrogel with its hydrophilic properties. The amide group on NIPAam is what provides the hydrogel with its thermal response characteristics. These amide groups undergo coil to globular transitions that contract the entire matrix much like the coils in proteins with the exact same amide groups. TEMED and APS are a part of the initiator complex. As TEMED is a catalyst, it only lowers the activation energy for the reaction and is theoretically recoverable.

Prepared using BKChemTool.

Outlined in procedure, the steps to make the hydrogel samples are:

1- Mix NIPAam, butenediol EGDMA and TEMED in pre gel solution with APS initiator complex. For fast polymerizations, preheat the pre-gel solution with a hot plate set to approximately 50 °C.

2- Once mixed, stir lightly for 5 seconds and prepare to pour into molds. Hot polymerizations will be done within 2.5 minutes and cold polymerizations must be left in the mold overnight.

3- Remove samples from molds and wash in a sonicator bath on de-gas for 15 minutes.

4- Soak samples in water and cycle on heat at approximately 45 °C until the thermal response is activated at least 10 times with an intermission soak each time.

5- Load with testing solution overnight on last heat cycle.

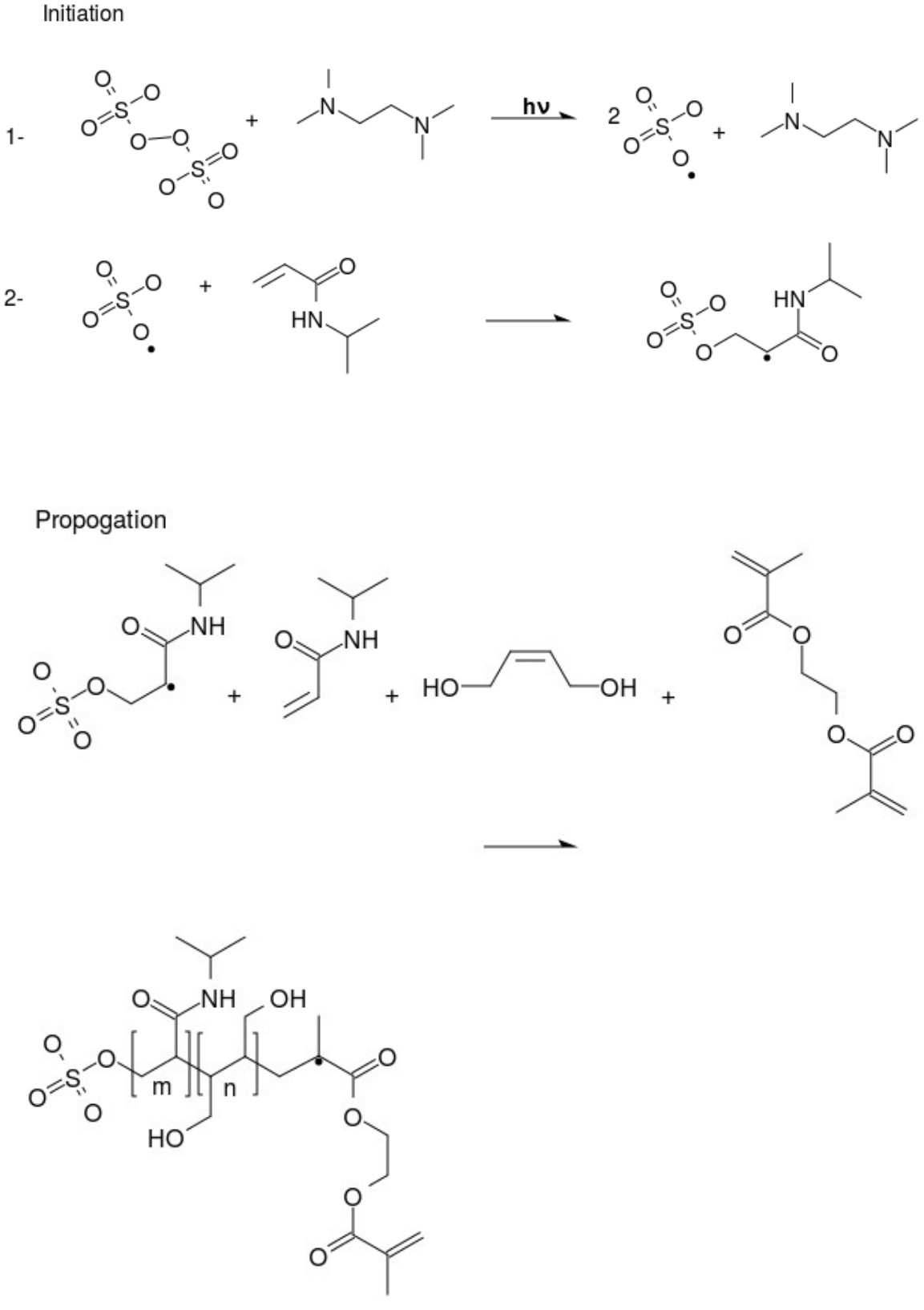

Illustration 3 (a): A diagram of the initiation and propagation reaction mechanisms for hydrogel synthesis

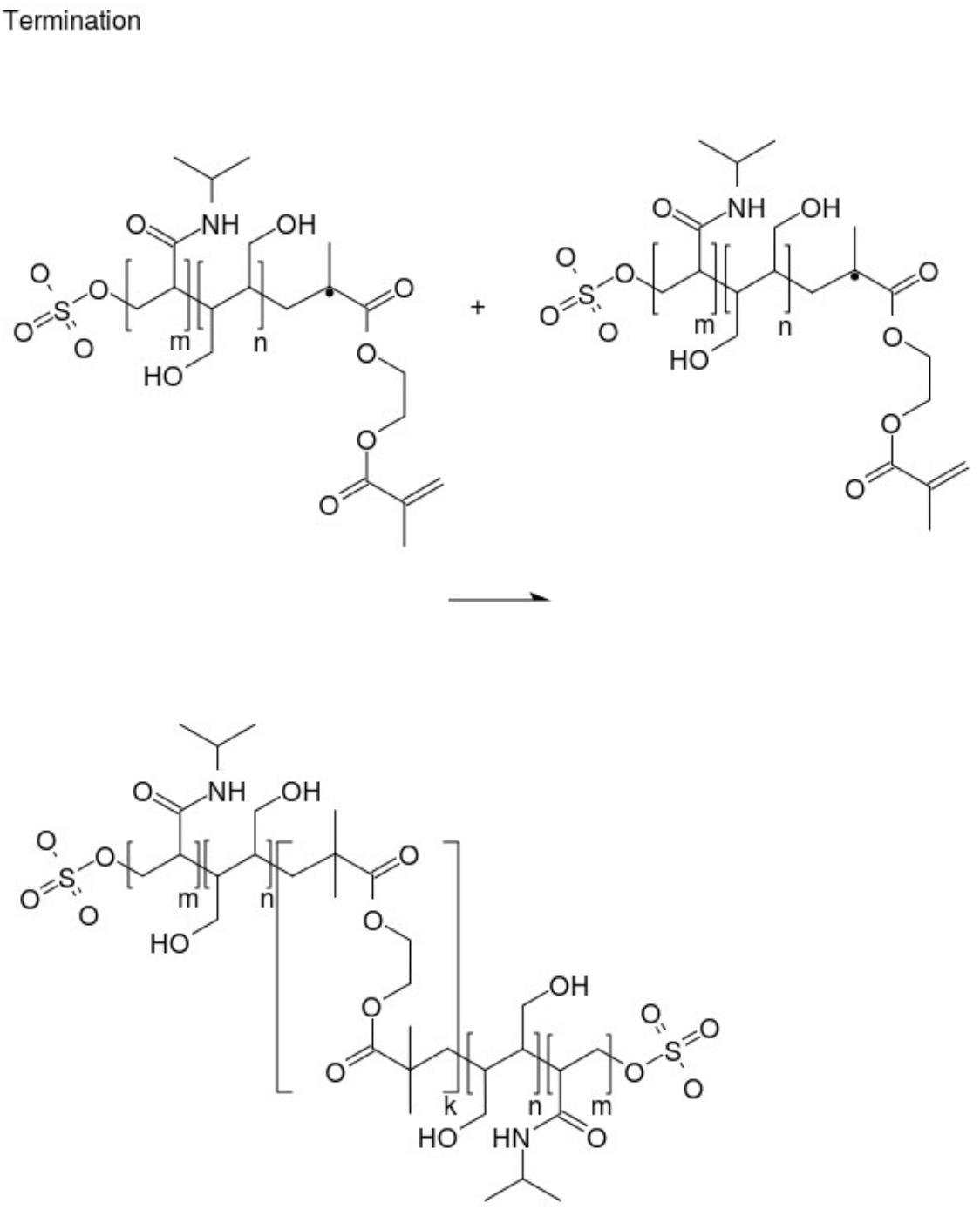

Illustration 3 (b): A diagram of the termination reaction mechanism and the formed hydrogel polymer matrix.

Heating Element

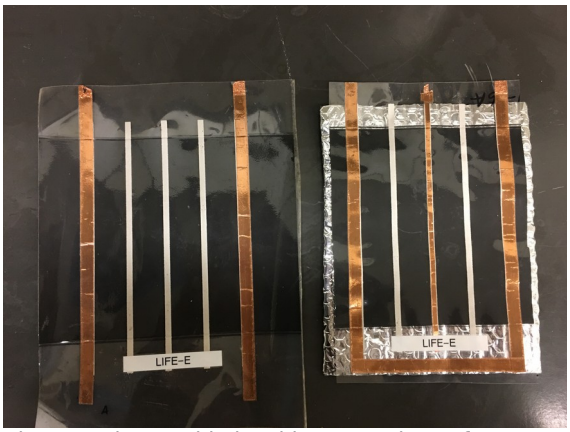

Photograph 1: A side by side comparison of two separate heating elements. On the left, a series resistor requires only two electrodes. On the right, two electrodes are still used however their topology makes a parallel circuit.

There is a wide variability in the potential resistance a given sheet of Nanoxene may have. Rather than characterizing sheet resistivity and modeling each heating element for optimization before fabrication, it is simpler to make a long sheet and cut the material to size for the intended application. Individual sheets are then tested for their internal resistance empirically. Sheets could then be set into efficiency bins which would translate to higher or lower priced heating elements. One caveat to this is that an order of magnitude control of the overall sheet resistance can be achieved given the geometry and number of electrodes used. Ideally, using copper wire and a parallel circuit for electrodes results in resistances that are much lower than those of similar sheet resistors that use serial electrodes. The parallel electrodes consistently draw more current and reach higher temperatures in shorter times. Refer to table 2 below for pertinent information on the circuit diagram and components. Refer to Photograph 1 for an image of 2 Nanoxene sheet resistors prepared at Life-E LLC Laboratories.

Component	**Max Voltage**	**Max Current**	**Max Power Drop**	**Internal Resistance**
Nanoxene				9.68 ohms
Arduino	5 V	40 mA	0.2 W	125 ohms
TIP-120	60 V	14 A	45 W	0.5 ohms

Table 2 : A collection of electrical components used in the circuit and some of their voltage characteristics.

Circuitry and Programming

Using an Arduino breadboard, a proto-circuit can be designed and used to test and debug code in sections. The first debugging phase involves optimizing the thermostat response code. This is achieved by first defining the floating pins and testing inputs and output displays on the serial monitor. Once the preferred responses are received by the thermostat, the data output will be coupled to another section of the circuit board. In particular, the output from the thermostat must be utilized to control the solid state relay switch. Once the switch relay deactivates upon the required input from the thermostat, optimizing the user interface control module is the last thing necessary to accomplish. A push button, and a few LEDs to display the operation mode are all that are required for optimization here. Now, coupling the response of the circuit to the output from the thermostat and the push button circuit is what allows for the definition of operation modes. The selection structures used in Arduino C+ require if/else loops and boolean logic operators. For example:

```
if((dC>=45.0)&&(bpc==2)){ // If the temp exceeds 45 and the counter is set to 2
        Serial.print("COOL DOWN MODE:  "); // Enter cool down mode
        Serial.print("CELSIUS  "); // Display temperature
        Serial.println(dC); // Degrees Celsius
        digitalWrite(l1p,HIGH); // Turn on LED 1
        digitalWrite(l2p,LOW); // Turn off LED 2
        digitalWrite(l3p,LOW); // Turn off LED 3
        digitalWrite(rlp,LOW); // Turn off load resistor
}
```

Displayed above is a section of code from the proto-control code. The green letters are notes left for others to understand and debug the code later. Letters in magenta are strings that are displayed as outputs on the serial monitor. The black letters represent command functions in Arduino C+. The blue "if" at the beginning is the initial boolean selection structure function. It allows the Arduino circuit to perform operations given certain initial criteria. These criteria are defined with boolean logic with the characters >= (greater than or equal to), == (equal to), and && (and only if). As a sentence, the operation would read "*if dC is greater than or equal to 45, and only if bpc is equal to 2, do: x, y, and z.*" The power of these functions is multifaceted: only one microcontroller switch is required to discriminate between and perform a multitude of operational modes, and multiple inputs can be used to define a single operational mode. This increases computational speed as only one clock needs to be referenced. It also clearly reduces costs in that respect. It also allows for the implementation of safety protocols in other devices that require users to shut safety screens or bay doors before activating a device.

Results and Discussion

Hydrogels

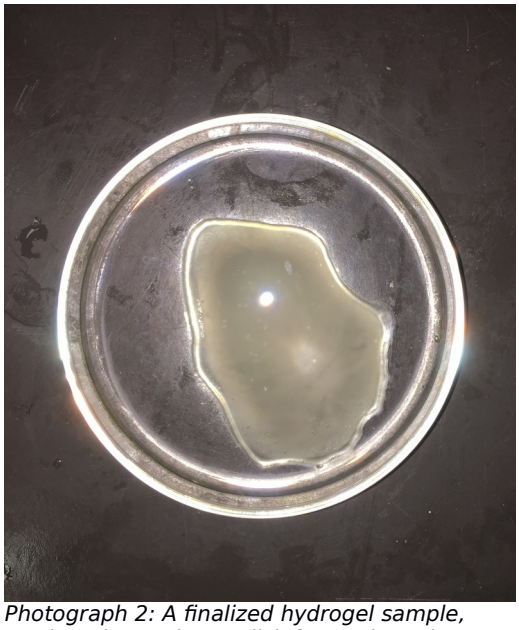

Photograph 2: A finalized hydrogel sample, ready to be cut into a disk for testing. The uniform opacity indicates no phase separations occurred during polymerization.

The best hydrogel samples used THF as the initial solvent, had EGDMA concentrations at 1.5 %mol, and used cold polymerizations over 24 hours to fully cure the hydrogels with molecular imprinting. This is due to THF being a strong organic solvent that is used commonly for dissolving amide structures like NIPAam or proteins. THF makes for a homogeneous and uniform pre-gel solution prepared for polymerization. After polymerization, THF is easily removed and replaced with any desired solvent loaded with medicine. The release kinetics of cold polymerizations are clearly superior. The hot polymerization samples all underperformed in release kinetics compared to the cold polymerization samples. Their only redeeming quality was the speed at which the reactions occurred, requiring less than 5 minutes to fully cure. Refer to Photograph 2 for an image of a finalized cold hydrogel sample.

The monomers butenediol and NIPAam display a gap in miscibility at the polymerization temperatures

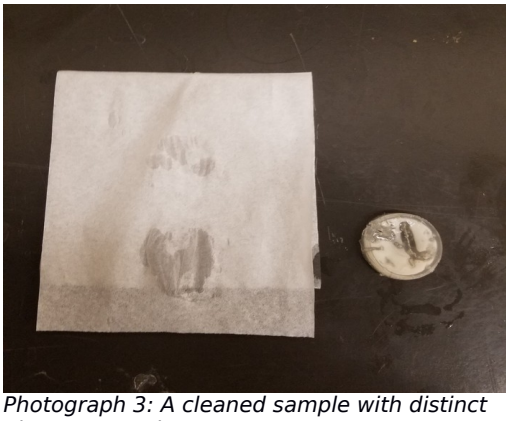

Photograph 3: A cleaned sample with distinct phase separations.

investigated here. This translated to failed polymerization attempts that were non-uniform, with phase separations that lead to rapid deterioration of the hydrogels in pre-gel solutions of distilled water and to some extent in acetone. Refer to Photograph 3 for an image of the phase separations in one sample. Polymerizations in water for the most part displayed the unwanted phase separations with broken chains and oligomers suspended in the matrix. Acetone required more diluted pre-gel concentrations than THF did to keep phase separations from occurring. THF pre-gel solvent consistently made better hydrogels with uniform polymerizations. This is due to the polar-aprotic solvent qualities of THF. It is commonly used for this reason in biological solvation reactions for proteins. NIPAam acts like a protein polypeptide when polymerized due to its amide functional groups, making THF an exceptionally effective solvent here.

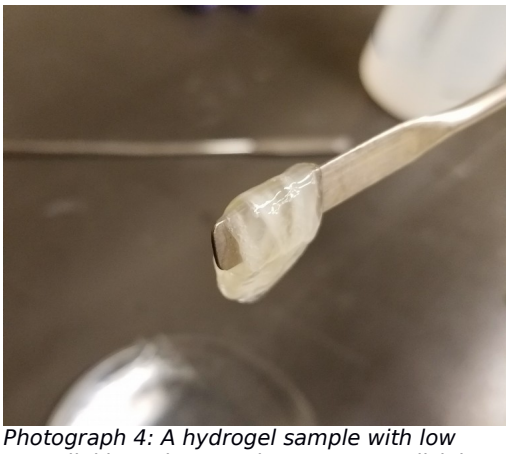

Photograph 4: A hydrogel sample with low cross linking. The sample was once a disk but has deformed over a thin spatula.

Varying the concentration of EGDMA had a wide array of effects on the qualitative mechanical properties of the gel samples. Samples at 1 %mol EGDMA were very weak with relatively low viscosities compared to firmer gel samples. These samples failed to make it past washing steps and deteriorated during step 3, the sonicator wash. Refer to Photograph 4 for an image of a hydrogel with a low degree of cross linking. On the other hand, the hydrogel samples at 2 %mol EGDMA and greater all were too brittle and hard or did not have the necessary thermal response characteristics. This is because cross-linking inhibits the coil to globular transitions necessary for thermal response by fixing chains firmly in place. Thermal responses consistently took longer, and hysteresis, caused by remanent globular transitions, were left behind. This means that the relaxation of the conformational transitions in the hydrogel takes longer to occur. Ideal mechanical properties were qualitatively observed at approximately 1.5 %mol concentrations of EGDMA.

The polymerizations at low temperatures (20 ^{o}C) required longer polymerization times. Hydrogels were allowed to cure overnight for 24 hours before being removed from glass molds. Refer to Photograph 5 for an image of one of the makeshift molds used to make samples. Faster polymerization times of approximately 5 minutes to fully cure were achieved with higher temperatures (50 ^{o}C). This is because higher temperatures provide the necessary kinetic energy to speed up the polymerization reaction. However, the data showed that only molecular imprinting with hydrogels at lower temperatures during polymerization is possible. This is because the Van-Der-Waals attractive forces that lead to molecular imprinting are decomposed at higher temperatures. This means that the “hot” gels did not have the necessary docking centers that allowed for more solute to fill the hydrogel and be released during the thermal response. UV-Vis spectrophotometry proved that the “cold” gel had an order of magnitude greater concentration of solute in the cuvette after the temperature response. Analysis with the Beer

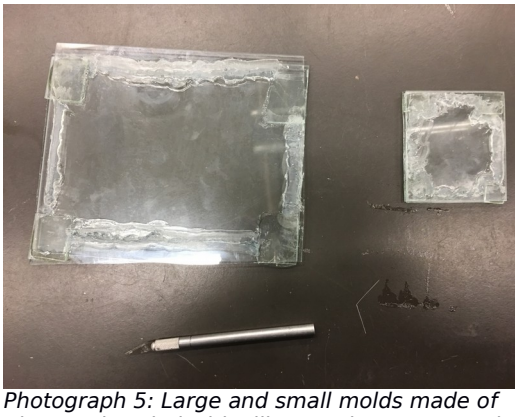

Photograph 5: Large and small molds made of glass and sealed with silicone. They were made by stacking glass plates. They were carefully opened by cleaving the silicone off one face only, leaving the silicone behind to act as a seal.

Lambert Law assumed that the molar absorptivity of lidocaine at 23,623 $Lmol^{-1}cm^{-1}$ the only characteristic absorptivity at play in the cuvette. This may not be the case as expelled oligomers may interact with light as well, skewing the data. Refer to illustration 4 for a display of the graphs and data from the UV-Vis scans and the integration data. It shows clearly higher concentrations after the temperature activation step that happens at 20 minutes. Though it cannot be said with certitude that what was released and recorded was purely the target molecule lidocaine, it is still clear that there are increases in absorbance with respect to temperature response in these samples. Therefore, thermal activation was still displayed in both samples.

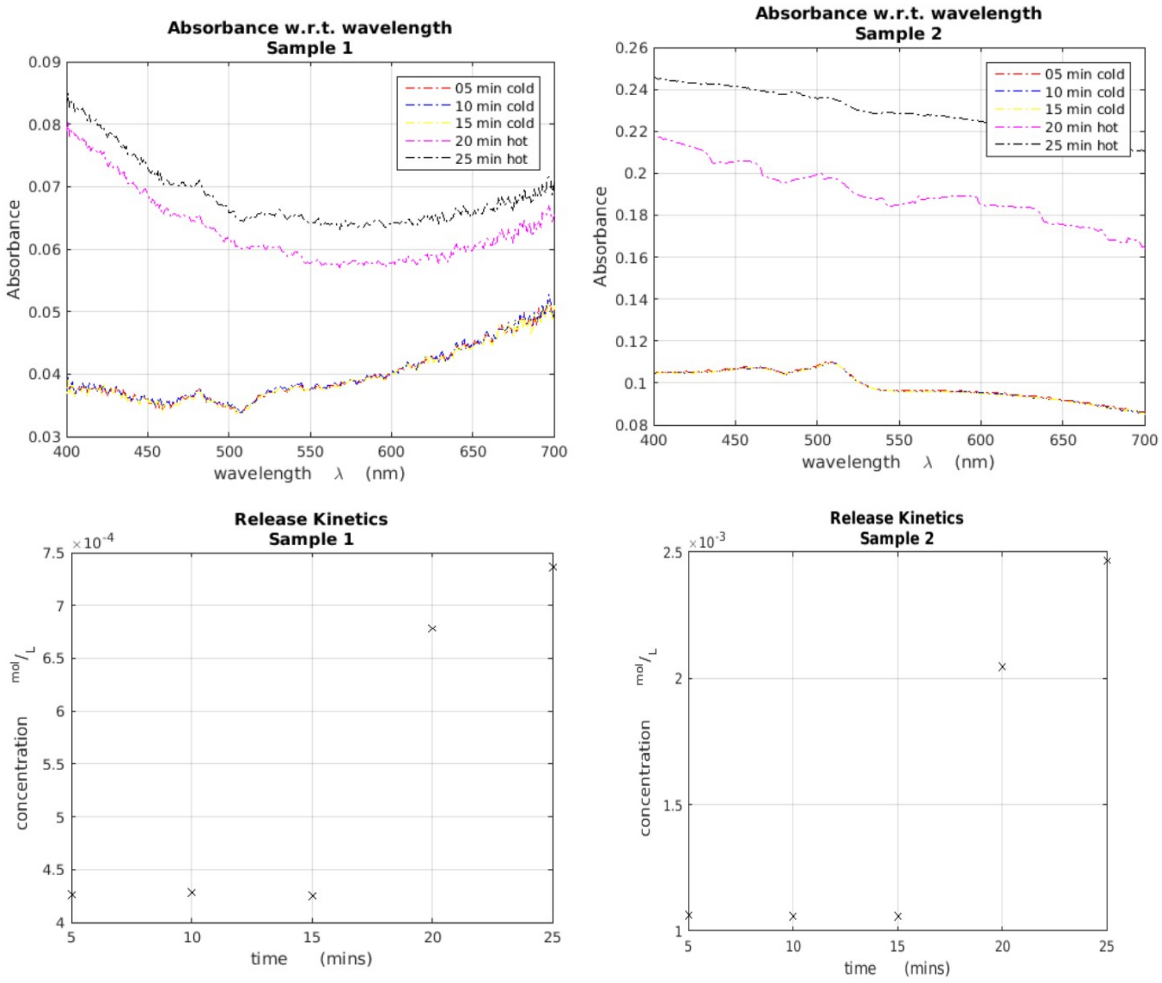

Illustration 4: A side by side comparison of absorbance data for molecular imprinting in hydrogels. Sample 2 was a "cold" gel and had greater release kinetics at the response time of 20 minutes. This can be seen from the integrated data showing increases in concentrations clearly at the 20 minute mark where temperature was increased.

One sample with 1 %mol butenediol, and 5 %mol EGDMA in THF solvent was left on heat overnight for its polymerization reaction. In the morning, the sample vial had a yellowed hydrogel sample with a collection of what was believed to be crystalline amide dendrites growing on the surface of the sample vial. This sample was an abject failure. However, the failure elucidated some interesting shortcomings of the heated polymerizations. Refer to Photograph 6 for an image of the crystals in the sample vial. In particular, the vapor pressure of THF increases greatly around 50 ºC as this is near its boiling point. As THF vaporizes, it also carries broken surface oligomers and free radicals in its vapor phase. These molecules undergo a surface vapor deposition at nucleation sites on the surface of the glass vial, making crystals. In order to avoid this in future polymerizations, the heat was adjusted to 30 ºC and allowed to heat for longer periods. This still provided the necessary kinetics for rapid polymerizations, although it remains to be seen what the temperature effects during polymerization on the release kinetics are.

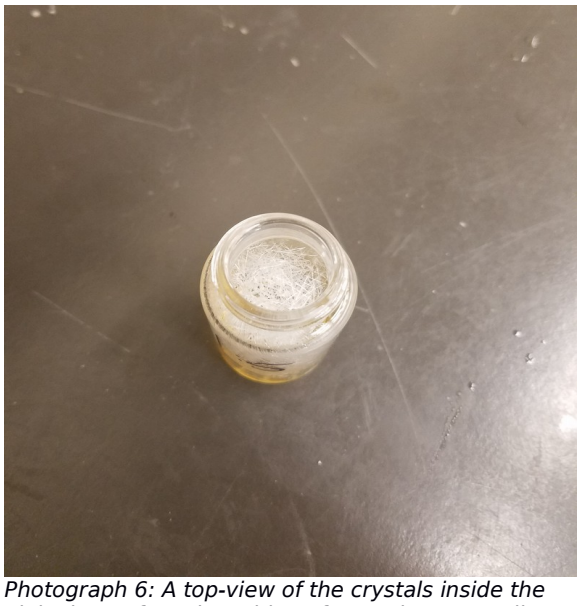

Photograph 6: A top-view of the crystals inside the vial. The surface deposition of crystals grew as linear dendrites. This follows from first order growth characteristics of the crystals from Avrami kinetics.

Shortcomings in value notwithstanding, the amide crystals were still characterized to better understand the crystallinity and chemical composition of these crystals. These crystals were thought to be made primarily of P-NIPA as NIPAam was initially at 99 %mol concentration for the reaction, however this still had to be confirmed. FTIR spectroscopy scans use infrared radiation absorption to identify the presence of certain types of bonds in a sample[11]. The crystals were analyzed using FTIR and displayed amide peaks and carbonyl peaks characteristic of NIPAam as well as carbon σ bonds. However, peaks for carbon π bonds are missing from the scan. This is indicative of NIPAam losing its carbon π bonds during polymerization, becoming P-NIPA. XRD scans at glancing angles with a zero diffraction background were also performed in an attempt to define its crystalline lattice structure. Refer to illustration 5 for a display of both the FTIR scan data and the XRD scan data alongside each other. Although they represent separate parts of the electromagnetic spectrum, they are both still, in essence, scans of interactions a sample has with various forms of light. XRD uses x-ray diffraction and constructive wave interference to define interplanar spacing in a crystalline sample. The zero diffraction background is a special stage designed to not interact with the x-ray signals used for elastic scattering. This increases weaker signals from low yield samples or a sample with a crystallinity that may be difficult to resolve. An amorphous sample will not have any peaks in its XRD scan as there will be no coherent atomic planes in the sample which will satisfy the conditions necessary for constructive interference. However crystals with ordered planes will display peaks at angles which correspond to indexed planes. The crystalline sample had a wide range of peaks with the lowest starting at less that 10 degrees of incidence. Low peaks are indicative of large lattice constants which are common to crystalline amides. There were no scans in literature or any crystallographic database to compare these scans to which would provide data on peak shifting

and peak broadening on the sample in the case of XRD. Therefore, the characterization of these crystals ended here.

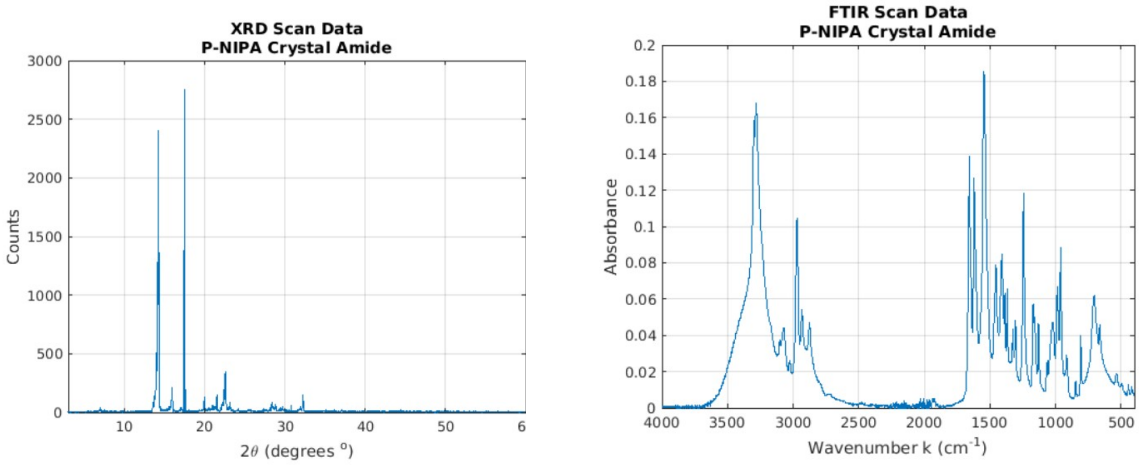

Illustration 5: A side by side comparison of FTIR and XRD data. FTIR displays the wavenumber on the x-axis and absorbance on the y-axis. It measures the amount of light at a given wavenumber that is absorbed, which is characteristic of a certain type of bond. XRD has the scattering angle on the x-axis and the photon counts on the y-axis. It measures the intensity of a diffraction angle at constructive interference to deduce interatomic spacing and crystal structure. FTIR requires a spectrum of incident light and takes advantage of photon absorption. XRD utilizes one wavelength and elastic photon scattering.

Slip rheometry measurements showed that the hydrogels were fully elastic with loss moduli and loss tangents that were consistently negligible throughout the entire frequency range studied. Fresh hydrogel samples could not be assessed in the machine due to time constraints. However the samples tested were preserved from previous polymerizations for two weeks and kept hydrated until the tests were done. Refer to Photographs 7 and 8 for images of the slip rheometer and of a loaded hydrogel sample. Discs of 20 mm radius and 3 mm thickness were cut for the machine and loaded at 1 N compressive force for the test. For all frequencies, the shear modulus G was consistently placed at approximately 3880 Pa with a near negligible standard deviation. This means the hydrogels are well within the safety factors required for mechanical strength in this application. These values are well above what is expected in literature from soft gels and are more comparable to tougher, firm gels reported in literature[13]. Using this shear modulus calculation, the total average cross linking density can be derived. Modeling the shear modulus magnitude as a linear scaling relationship with atomic activation energy and the cross

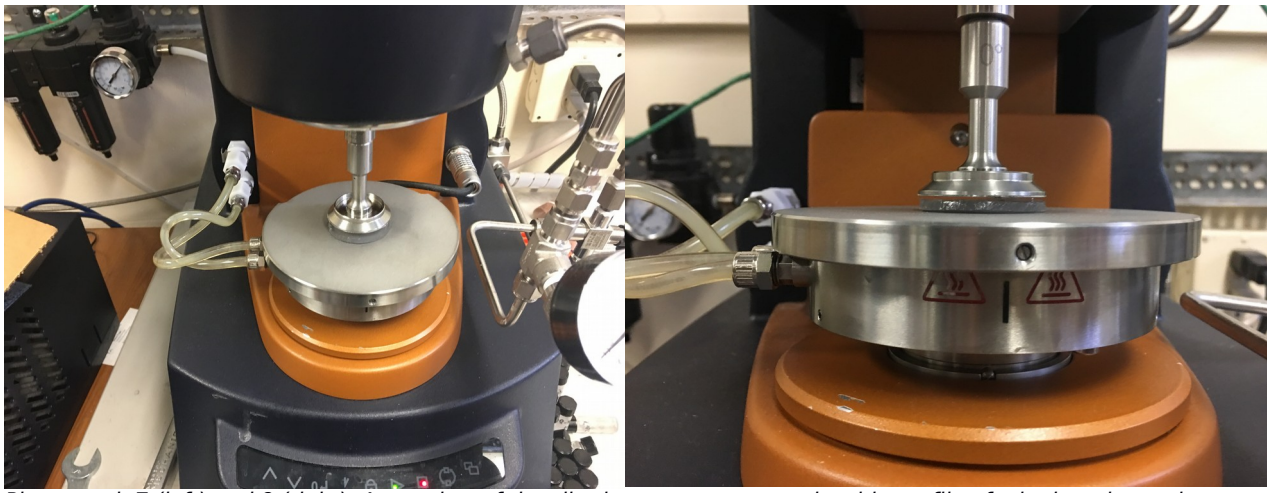

Photograph 7 (left) and 8 (right): A top-view of the slip rheometer stage and a side profile of a hydrogel sample on the stage on the left. On the right, the testing probe comes to rest on the sample for testing from the top and applies torsion to the sample. Varying the velocity at which the torsion is applied is how dynamic strain testing is performed.

linking density is a simple and easily accessible calculation. It allows us to derive the cross linking contribution to the shear modulus as atomic energy contribution. Normalized for a 1000 nm^3 unit volume, it is shown that there is on average, 1 cross link in a given 10 nm x 10 nm x 10 nm volume. Mechanical strength of the hydrogels was shown to change qualitatively depending on the solvent concentration in the gel during swelling. There could perhaps be an ideal concentration of medicine and solvent for mechanical strength in the gels that was not investigated further here. Refer to illustration 6 for a collection of graphs on the mechanical properties of the hydrogel samples and table 3 for a collection of metrics on the hydrogel samples.

Characteristics	**Values for Samples**	**Values reported by Chetty, A. et al[20]**
Storage Modulus G'	3881.56 Pa	1000-7000 Pa (3080 at lowest St. Dev)
Loss Tangent	~0	~ 15 for lowest value
Average Cross Linking Density	$\frac{1}{1000\,nm^3}$	

Table 3: A collection of metrics on the hydrogel samples and a comparison to other reported measurements for similar hydrogels. Unreported data are left as blank inputs in the table.

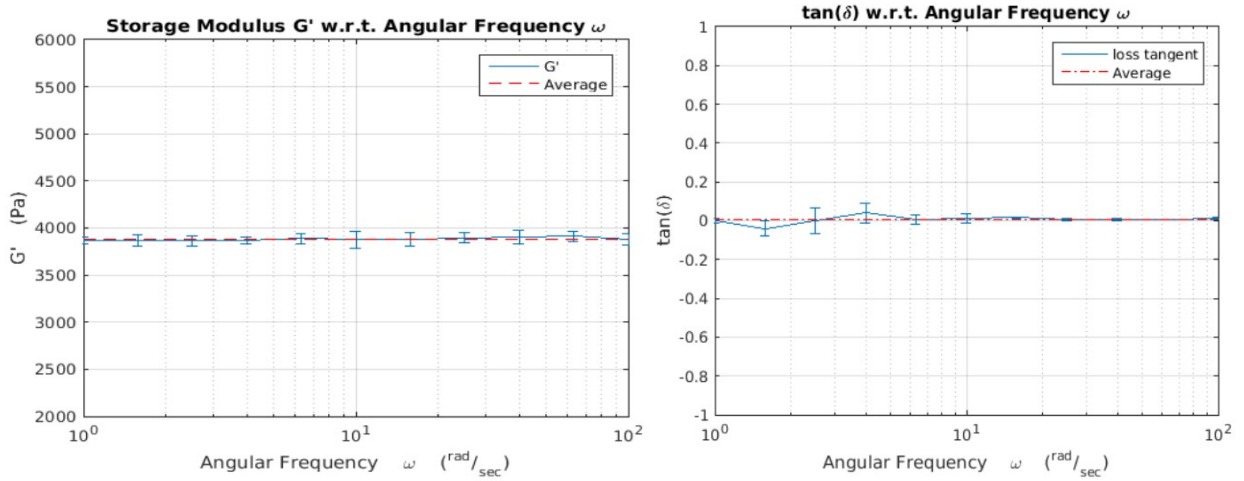

Illustration 6: A collection of graphs showing the storage modulus and loss tangent for the samples. The data is shown on logarithmic plots with errorbars to show certitude in measurements. A loss tangent that approaches zero means that there is little loss for a material, making it near perfectly elastic, which is expected for firm hydrogels.

Circuitry and Programming

The microcontroller performed its predefined tasks as it was programmed to do successfully. TIP-120 transistors proved to be effective in controlling and switching currents without overheating and failing. Although, there were issues at first with the circuit not being properly grounded, which led to the unnecessary debugging of the code over the course of a week. This was because the microcontroller pins were not laid out properly on the breadboard. In particular, a reference node pin, or grounding pin, from the microcontroller to the higher power circuit must be set regardless of the fact that these are, in essence, two completely separate circuits. The ground node pin senses a voltage on the other side, allowing the Arduino to

reference itself to it. Meaning that for a 5 V circuit, the ground node may be at 1 V and the max may be at 6 V. If the Arduino does not reference this to itself, it leaves its control pin as a floating pin and does not switch the higher current when the power activates. Once a ground pin was set, the switch worked as planned and the heating element powered up and powered down according to sensor inputs from the thermostat switch. Refer to Photograph 9 for an image of the Arduino circuit without the external battery or heating element connected. Once the circuit was amended with the necessary grounding wire, the circuit and programming functioned accordingly.

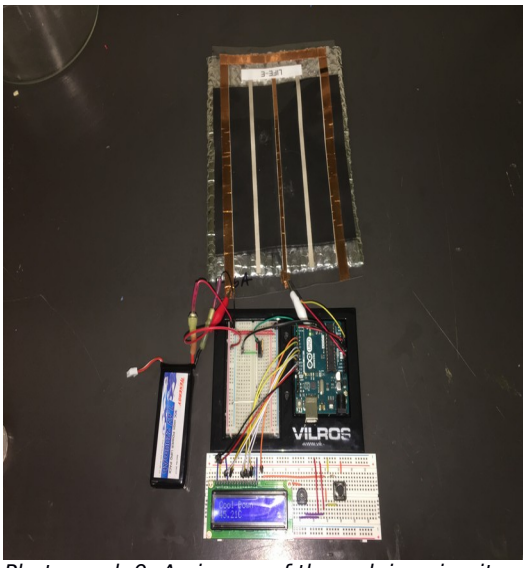

Photograph 9: An image of the arduino circuit which controls the heating element seen at the top. At the middle, a high power breadboard controls the heater and the arduino. Below, a low power breadboard controls the interface control module and protects the low power elements. The thermostat sensor goes up and under the Nanoxene heating element to measure temperature.

Circuit voltages at 7 V and 14 V were tested prior to battery testing with a DC signal generator. Load characteristics were read from the generator screen and showed a linear increase of current draw as is expected. The 14 V circuit heated faster and turned off more often than did the 7 V circuit. However, the 7 V circuit had no problems reaching its predefined operating temperatures and switching off when it reached them. Powering the circuit with a 14 V bias was therefore found to be unnecessary. The battery used to power the portable version of the prototype was a 7.4 V Li-Po RC battery. It worked successfully and had operating times that exceeded one hour between charges. Further testing on maximum battery and operation life were not performed as this would clearly change with the type of battery implemented. A final product would have one either set inside or have a removable battery pack that could be charged separately. Ultimately, this concern did not fit into the scope of the rapid prototyping aspect of the design project.

Integration

After each component had been optimized and individually completed, using various adhesives to fix the hydrogel layer to the heating element were investigated. Nanoxene, at its operating temperature, provided the necessary activation energy for thermal response in the hydrogels and was capable of pairing with adhesive layers. However, fixing the hydrogel to the mylar sheet surface on the heating element proved to be too difficult and was abandoned here. The adhesives used were not water proof or took far too long to cure and allowed the hydrogel to dry out. At first, double sided tape was used to set dry samples that were loaded with solution afterwards. This did not succeed as the tape washed off during loading and the samples came free. Afterwards, using silicone sealant was attempted as it is waterproof and sets under water. This failed as well due to the length of time it takes for the silicone to cure. The samples began to dry before ever being attached to the heating element. The approach used to fix the hydrogel to the surface was flawed in that it called for the wrong adhesives, for the wrong procedures in properly curing the adhesives, and perhaps even a flawed architecture. Further attempts to fix the hydrogels to Nanoxene were abandoned here due to time constraints at the end of this design.

Conclusion

The most effective NIPAam hydrogel samples all used THF as an initial solvent and were polymerized over 24 hours at room temperature. The major requirements for uniform polymerizations and synthesis of hydrogels are:

1. Uniform and homogeneous pre-gel solutions of peak concentration.
2. Room temperature polymerizations with 24 hours cure time.
3. Low amounts of initiator complex and optimized cross linker concentrations.
4. Optimized solution loading and swelling characteristics after polymerization.

The hydrogel samples all displayed thermal responses that were favorable for the intended application, with release response kinetics in a temperature range that is effective for the combined utilization of thermotherapy. The hydrogels also displayed potential capabilities in molecular imprinting, with an order of magnitude greater release concentrations after thermal response.

The circuit controlled the heating element as designed and provided an operational lifetime that was greater than one hour during experiments. This could change depending on the battery used. It is possible that longer operation lifetimes between charges could be achieved by using a simpler control display module. The LCD screen used here was effective in showing the actual operational mode and current temperature, however this will most likely be unnecessary in a final prototype. Utilizing a few LEDs instead will increase operational lifetimes as they will draw less current and require less power than the LCD.

In future experiments, the design should consider further testing the effects of initial polymerization temperature on the release kinetics on these samples. Thorough testing for a reliable standard deviation should include testing 100-1000 samples over the course of 6 months. This will provide a better understanding of the release kinetics and mechanical properties of the hydrogels. Investigating other adhesives such as gum adhesive that could be integrated perhaps during polymerization should be considered. They could serve to bond the surfaces of the heating element and the hydrogel together better. Functionalizing the surface of the mylar sheet with chemicals that can participate in bonding with the hydrogel should be investigated as well.

Moving forward, investigating how to minimize electronics for future prototypes should be considered. Although Arduinos are user friendly, they are bulky and expensive. Using a PCM-32 microcontroller or using a simple voltage regulator circuit with an operational amplifier to control the feedback response loop would go a long way to minimizing costs during prototyping. The final cost reductions would come from hiring a larger company to print integrated heating circuits for the final product, and from making hydrogels in bulk. Preferably, developing a tape casting process that integrates the hydrogel layer into Nanoxene at the start should be done with a team of process engineers.

References

[1] Petrofksy, J., Berk, L., et.al. December 01, 2013. “Moist Heat or Dry Heat for Delayed Onset Muscle Soreness” Journal of Clinical Medical Research, 5(6), 416–425. [Web Accessed October, 2017: University of Utah Marriott Library Research Database]

[2] Weingand, K., Hengehold, D., et.al. May, 1999. “Topical Heat Provides Pain Relief of Delayed Onset Muscle Soreness of the Distal Quadricep Muscles” Medicine & Science in Sports & Exercise Issue: Volume 31(5) Supplement, May 1999, p S75 [Web Accessed October, 2017: University of Utah Marriott Library Research Database]

[3] Author Unknown, April 19, 2017. “Capsaicin Topical” University of Michigan. Published by Michigan Medicine [Web Accessed February, 2018: Google Search] <http://www.uofmhealth.org/health-library/d01321a1>

[4] Strauss, W.A., January 1, 2008. “Partial Differential Equations: An Introduction” Wiley Publishing. Brown University

[5] Gutowska, A. “Heparin Releasing Thermosensitive Hydrogel” The University of Utah Doctor of Philosophy Department of Pharmaceutics and Pharmaceutical Chemistry December 1994

[6] Corish, J., Corrigan, O.I., January 1, 1990 “Transdermal Diffusion of Drug Molecules” Journal of Chemical Society on Faraday Transformers. Trinity College Department of Chemistry. Dublin, Ireland. [Web Accessed February, 2018: University of Utah Marriott Library Research Database]

[7] Ganji, F, Vasheghani-Farahani, E. “Hydrogels in Controlled Drug Delivery Systems” Chemical Engineering Department, Faculty of Engineering Tarbiat Modares University, P.O. Box: 14115-143, Tehran, Iran

[8] Dı´ez-Pen, E. et al. “Thermal Properties of Cross-Linked Poly(N-isopropylacrylamide) [P(N-iPAAm)], Poly(methacrylic acid) [P(MAA)], Their Random Copolymers [P(N-iPAAm-co-MAA)], and Sequential Interpenetrating Polymer Networks (IPNs)” Departamento de Quı´mica-Fı´sica de Polı´meros, Instituto de Ciencia y Tecnologı´a de Polı´meros,C.S.I.C., Juan de la Cierva 3, E-28006 Madrid, Spain, and Departamento de Farmacia y Tecnologı´a Farmace´utica, Facultad de Farmacia, UCM, Avenida de la Complutense, E-28040 Madrid, Spain Received August 23, 2001

[9] Gaskell, D.R., January 1, 2012 “An Introduction to Transport Phenomena in Materials Engineering, Second Edition” Momentum Press, LLC.

[10] Whitcombe, M.J., Kirsch, N. Nicholls, I.A., June 1, 2014. “Molecular imprinting science and technology: a survey of the literature for the years 2004–2011” Journal of Molecular Recognition Volume 27, Issue 6 Pg. 297-401 [Web Accessed October, 2017: University of Utah Marriott Library Research Database]

[11] Carey, F.A., Giuliano, R.M., January 1, 2011 “Organic Chemistry, Eighth Edition” Published 2011 McGraw Hill, LLC.

[12] Gere, J.M., Goodno, B.J., January 1, 2013 “Mechanics of Materials, 8th Edition” Published 2013 Cengage Learning, LLC. pp.254-255

[13] Chetty, A. et al January 1, 2013, “A versatile characterization of poly(N isopropylacrylamideco-N,N'-methylene-bis-acrylamide) hydrogels for composition, mechanical strength, and rheology”, Express Polymer Letters, 7, 1, pp. 95-105, [Web Accessed March, 2018: University of Utah Marriott Library Research Database]